Influence of pointlike disorder on the guiding of vortices and the Hall effect in a washboard planar pinning potential

Valerij A. Shklovskij
Institute of Theoretical Physics, National Science Center-Kharkov Institute of Physics and Technology, 61108, Kharkov, Ukraine and Kharkov National University, Physical Department, 61077, Kharkov, Ukraine

Oleksandr V. Dobrovolskiy
Kharkov National University, Physical Department, 61077, Kharkov, Ukraine

(Received 23 February 2006; revised manuscript received 27 July 2006; published 27 September 2006)

Explicit current-dependent expressions for anisotropic longitudinal and transverse nonlinear magnetoresistivities are represented and analyzed on the basis of a Fokker-Planck approach for two-dimensional single-vortex dynamics in a washboard pinning potential in the presence of pointlike disorder. Graphical analysis of the resistive responses is presented both in the current-angle coordinates and in the rotating current scheme. The model describes nonlinear anisotropy effects caused by the competition of pointlike (isotropic) and anisotropic pinning. Nonlinear guiding effects are discussed, and the critical current anisotropy is analyzed. Gradually increasing the magnitude of isotropic pinning force this theory predicts a gradual decrease of the anisotropy of the magnetoresistivities. The physics of the transition from the new scaling relations for anisotropic Hall resistance in the absence of pointlike pins to the well-known scaling relations for the pointlike disorder is elucidated. This is discussed in terms of a gradual isotropization of the guided vortex motion, which is responsible for the existence in a washboard pinning potential of new (with respect to magnetic field reversal) Hall voltages. It is shown that whereas the Hall conductivity is not changed by pinning, the Hall resistivity can change its sign in some current-angle range due to presence of the competition between i and a pins.

DOI: 10.1103/PhysRevB.74.104511 PACS number(s): 74.25.Fy, 74.25.Sv, 74.25.Qt

I. INTRODUCTION

The importance of flux-line pinning in preserving superconductivity in a magnetic field has been generally recognized since the discovery of type-II superconductivity. But until now the mechanism of flux-line pinning and creep in superconductors [and particularly in the high-T_c superconductors (HTSC's)] is still a matter of controversy and great current interest, especially in the cases of strong competition between different types of pins.

One of the open issues in the field is the influence of *isotropic* pointlike disorder on the vortex dynamics in the *anisotropic* washboard planar pinning potential (PPP) for the case of arbitrary orientation of the transport current with respect to the PPP "channels" where the *guiding of vortices* can be realized. The importance of this issue may be substantiated by ubiquitous presence of pointlike pins in those high- and low-T_c superconductors which were used so far for resistive measurements of the guided vortex motion.[1–9]

The first attempt to discuss the influence of isotropic pointlike disorder on the guiding of vortices was made by Niessen and Weijsenfeld[1] in 1969. They studied guided motion *in the flux-flow regime* by measuring transverse voltages of cold-rolled sheets of a Nb-Ta alloy for different magnetic fields H, transport current densities J, temperatures T, and angles α between the rolling and current direction. The (H,J,T,α) dependences of the cotangent of the angle β between the average vortex velocity $\langle \mathbf{v} \rangle$ and the vector $\mathbf{J}$ direction were presented. For the discussion, a simple theoretical model was suggested, based on the assumption that vortex pinning and guiding can be described in terms of an isotropic pinning force $\mathbf{F}_p^i$ plus a pinning force $\mathbf{F}_p^a$ with a fixed direction which was perpendicular to the rolling direction. The experimentally observed dependence of the transverse and longitudinal voltages on the magnetic field in the flux-flow regime as a function of the angle α was in agreement with this model.

Unfortunately, in spite of the correct description of a geometry of the motive forces of a problem (see below Fig. 1) it was impossible within the flux-flow approach[1] to calculate

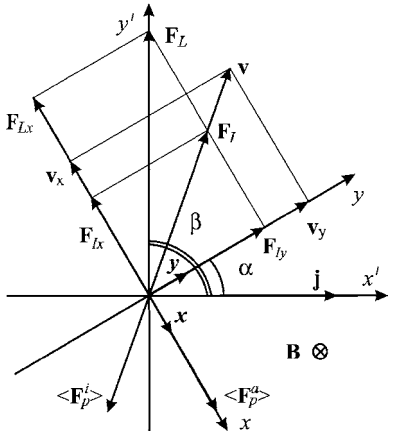

FIG. 1. System of coordinates xy (with the unit vectors $\mathbf{x}$ and $\mathbf{y}$) associated with the PPP planes and the system of coordinates $x'y'$ associated with the direction of the current density vector $\mathbf{j}$; α is the angle between the channels of the PPP and $\mathbf{j}$, β is the angle between the average velocity vector of the vortices $\mathbf{v}$ and the vector $\mathbf{j}$, $\mathbf{F}_L$ is the Lorentz force, $\langle \mathbf{F}_p^i \rangle$ and $\langle \mathbf{F}_p^a \rangle$ are the average isotropic and anisotropic pinning forces, respectively, and $\mathbf{F}_I$ is the average effective motive force for a vortex. Here for simplicity we assume $\epsilon=0$.

theoretically the *nonlinear* (J,T,α) dependences of the average pinning forces $\langle \mathbf{F}_p^i \rangle$ and $\langle \mathbf{F}_p^a \rangle$ which determine the experimentally observed cot $\beta(J,T,\alpha)$ dependences.

The *nonlinear guiding* problem was exactly solved at first only for the washboard PPP (i.e., for $\mathbf{F}_p^i=0$) within the framework of the two-dimensional single-vortex stochastic model of anisotropic pinning based on the Fokker-Planck equation with a concrete form of the pinning potential.[10,11] Two main reasons stimulated these theoretical studies. First, in some HTCS's twins can easily be formed during the crystal growth.[2–5,8] Second, in layered HTCS's the system of interlayers between parallel *ab* planes can be considered as a set of unidirectional planar defects which provoke the intrinsic pinning of vortices.[12]

Rather simple formulas were derived[11] for the experimentally observable *nonlinear* even (+) and odd (−) (with respect to the magnetic field reversal) longitudinal and transverse magnetoresistivities $\rho_{\parallel,\perp}^{\pm}(j,\theta,\alpha,\varepsilon)$ as functions of the dimensionless transport current density j, dimensionless temperature θ, and relative volume fraction $0<\varepsilon<1$ occupied by the parallel twin planes directed at an angle α with respect to the current direction. The $\rho_{\parallel,\perp}^{\pm}$ formulas were presented as linear combinations of the even and odd parts of the function $\nu(j,\theta,\alpha,\varepsilon)$ which can be considered as the probability of overcoming the potential barrier of the twins[11]; this made it possible to give a simple physical treatment of the nonlinear regimes of vortex motion (see below, Sec. II C).

Besides the appearance of a relatively large even transverse $\rho_{\perp}^{+}$ resistivity, generated by the guiding of vortices along the channels of the washboard PPP, explicit expressions for *two new nonlinear anisotropic Hall resistivities* $\rho_{\parallel}^{-}$ *and* $\rho_{\perp}^{-}$ were derived and analyzed. The physical origin of these *odd* contributions caused by the subtle interplay between even effect of vortex guiding and the odd Hall effect. Both new resistivities were going to zero in the linear regimes of the vortex motion [i.e., in the thermoactivated flux flow (TAFF) and the ohmic flux flow (FF) regimes] and had a bumplike current or temperature dependence in the vicinity of highly nonlinear resistive transition from the TAFF to the FF. As new odd resistivities arose due to the Hall effect, their characteristic scale was proportional to the small Hall constant as for ordinary odd Hall effect investigated earlier.[10] It was shown[11] that appearance of these new odd $\rho_{\parallel,\perp}^{-}$ contributions leads to new specific angle-dependent "scaling" relations for the PPP which demonstrate the so-called anomalous Hall behavior in the type-II superconductors.

Here we should to emphasize that the anomalous behavior of the Hall effect in many HTSC's and in some conventional superconductors in the mixed state remains one of the challenging issues in the vortex dynamics.[5,12,13] This problem manifests itself experimentally by the Hall-effect sign reversal in the vortex state with respect to the normal state (at temperatures near T_c and for moderate magnetic fields) and the existence of the Hall resistivity scaling relation $\rho_{\perp} \sim \rho_{\parallel}^{\beta}$ with $1 \leq \beta \leq 2$, where $\rho_{\perp}$ is the Hall resistivity and $\rho_{\parallel}$ is the longitudinal resistivity. One of the main theoretical issues in the field is the influence of the pinning on the "Hall anomaly" and scaling relation. On the assumption that the "bare" Hall coefficient α_H is constant [see below, Eq. (1)], two different scaling laws have been derived earlier theoretically for different pinning potentials.[11,14] On the one hand, Vinokur *et al.* have shown[14] that a scaling law $\rho_{\perp}=\delta\rho_{\parallel}^2$ (where $\delta=n\alpha_H c^2/B\Phi_0$ is the Hall conductivity, $n=\pm 1$, c is the speed of light, B is the magnetic field and Φ_0 is the magnetic flux quantum) is the general feature of any isotropic vortex dynamics with an average pinning force directed along the average vortex-velocity vector. On the other hand, later it was shown[11] that for a washboard PPP, the form of corresponding scaling relation is highly anisotropic due to the reason that pinning force for *a* pins is directed perpendicular to the PPP channels. The scaling law for $\alpha=0$ has the form $\rho_{\perp}=-n(\alpha_H/\eta)\rho_{\parallel}$ (η is the vortex viscosity) which was interpreted previously[11] as a scaling law with $\beta=1$, whereas for $\alpha=\pi/2$ the scaling relation is more complex.[11] As it is shown in this paper, the $\rho_{\perp}^{-}$ resistivity for $(i+a)$ pins can be presented as a sum of the three contributions with the different signs. The graphical analysis in Sec. III of this paper represents a some range of the (α,j) values where the theory predicts a nonlinear change of the $\rho_{\perp}^{-}$ sign.

Let us consider another specific feature of the purely anisotropic guiding model.[10,11] From the mathematical viewpoint, the nonlinear anisotropic problem, as solved in Ref. 11, reduces to the Fokker-Planck equation of the one-dimensional vortex dynamics[15] because the vortex motion is unpinned in the direction which is parallel to the PPP channels. As a consequence, a critical current j_c exists only for the direction which is strictly perpendicular to the PPP channels ($\alpha=0$); $j_c(\alpha)=0$ for any other direction ($0<\alpha\leq\pi/2$). However, the measurements of the magnetoresistivity show[1–8] that $j_c(\alpha)>0$ for all α [although $j_c(\alpha)$ may be anisotropic]. So, in spite of some merits of a model with a washboard PPP, which was the first exactly solvable stochastic nonlinear model of anisotropic pinning, it cannot describe the j_c anisotropy of the experimentally measured samples.

Due to this reason, later another simple model was suggested,[16,17] which demonstrates this j_c anisotropy for all α on the basis of the bianisotropic pinning potential formed by the sum of two washboard PPP's in two mutually perpendicular directions. In contradistinction to the nonlinear model with uniaxial PPP,[11] this bianisotropic nonlinear model predicts a $j_c(\alpha)$ anisotropy and relates it to the guiding anisotropy, describing the appearance of two steplike and two bumplike singularities in the $\rho_{\parallel,\perp}^{+}$ and $\rho_{\parallel,\perp}^{-}$ (Hall) resistive responses, respectively. Although several proposals to realize experimentally this bianisotropic model were discussed so far,[16] the corresponding experiments, however, are still absent.

At the same time, the experimental study of vortex dynamics in the PPP is always accompanied by the presence of a certain level of pointlike disorder. So, as far as the analysis of existing experimental data is concerned, none of the present theoretical studies in the limiting cases of purely anisotropic or isotropic pinning are sufficient. The more general approach is needed.

The objective of this paper is to present results of a theory for the calculation of the nonlinear magnetoresistivity tensor at arbitrary value of competition between pointlike and anisotropic planar disorder for the case of in-plane geometry of

experiment. This approach will give us the experimentally important theoretical model which demonstrates the j_c anisotropy for all α and predicts a nonlinear change of the $\rho_{\perp}^{-}$ sign at some set of parameters (without change of the Hall *conductivity*) due to competition of the washboard PPP and a pointlike disorder.

The organization of the article is as follows. In Sec. II we derive main results of the $(i+a)$-pinning problem and consider two main limiting cases of purely a or i pinning. In Sec. III we represent the graphical analysis of different types of nonlinear responses—in particular, the (j,α) graphs of the $\rho_{\parallel,\perp}^{\pm}$ magnetoresistivities and the resistive response in a rotating current scheme. In Sec. IV we conclude with a general discussion of our results.

II. MAIN RELATIONS

A. Formulation of the problem

The Langevin equation for a vortex moving with velocity $\mathbf{v}$ in a magnetic field $\mathbf{B}=\mathbf{n}B$ $(B\equiv|\mathbf{B}|$, $\mathbf{n}=n\mathbf{z}$, $\mathbf{z}$ is the unit vector in the z direction and $n=\pm 1)$ has the form

$$\eta_0\mathbf{v}+n\alpha_H\mathbf{v}\times\mathbf{z}=\mathbf{F}_L+\mathbf{F}_p^a+\mathbf{F}_p^i+\mathbf{F}_{th}, \tag{1}$$

where $\mathbf{F}_L=n(\Phi_0/c)\mathbf{j}\times\mathbf{z}$ is the Lorentz force (Φ_0 is the magnetic flux quantum, and c is the speed of light), $\mathbf{F}_p^a=-\nabla U_p(x)$ is the anisotropic pinning force [$U_p(x)$ is the washboard planar pinning potential], $\mathbf{F}_p^i$ is the isotropic pinning force induced by uncorrelated point-like disorder, $\mathbf{F}_{th}$ is the thermal fluctuation force, η_0 is the vortex viscosity, and α_H is the Hall constant.

For purely isotropic pinning (i.e., for $\mathbf{F}_p^a=0$), Eq. (1) was earlier solved[14] for $\mathbf{F}_{th}=0$, using the fact that

$$\mathbf{F}_p^i=-\eta_i(v)\mathbf{v}, \tag{2}$$

where $\eta_i(v)$ is velocity-dependent viscosity and $v\equiv|\mathbf{v}|$.

Below we will show [see Eq. (8) and Sec. II D] that the solution, obtained in Ref. 14, can be presented in terms of the probability function of overcoming the effective current- and temperature-dependent potential barrier of isotropic pinning $\nu_i(F_I)$, which is simply related to $\eta_i(v)$.

In the absence of pointlike disorder (i.e., for $\mathbf{F}_p^i=0$), Eq. (1) was reduced to the Fokker-Planck equation, which was solved,[10,11] assuming that the fluctuational force $\mathbf{F}_{th}(t)$ is represented by a Gaussian white noise, whose stochastic properties are assigned by the relations

$$\langle F_{th,i}(t)\rangle=0,\langle F_{th,i}(t)F_{th,j}(t')\rangle=2T\eta_0\delta_{ij}\delta(t-t'), \tag{3}$$

where T is the temperature in energy units.

In what follows we derive the solution of Eq. (1), using for $\mathbf{F}_p^i$ the assumption (2), which reduces Eq. (1) to the equation

$$\eta\mathbf{v}+n\alpha_H\mathbf{v}\times\mathbf{z}=\mathbf{F}_L+\mathbf{F}_p^a+\mathbf{F}_{th}, \tag{4}$$

where $\eta=\eta(v)\equiv\eta_0+\eta_i(v)$. Using the result of Ref. 11, the self-consistent solution of the Eq. (4) can be represented as

$$\eta(v)\langle v_x\rangle=F_a\nu_a(F_a)/(1+\tilde{\epsilon}^2),$$

$$\eta(v)\langle v_y\rangle=F_{Ly}+n\tilde{\epsilon}F_a\nu_a(F_a)/(1+\tilde{\epsilon}^2), \tag{5}$$

where $\nu_a(F_a)$ is the probability of overcoming the PPP under the influence the effective moving force $F_a\equiv F_{Lx}-n\tilde{\epsilon}F_{Ly}$, F_{Lx} and F_{Ly} are the Lorentz force components acting along the vector $\mathbf{x}$ and $\mathbf{y}$, respectively, $\tilde{\epsilon}\equiv\epsilon Z(v)$, $\epsilon\equiv\alpha_H/\eta_0$, and $Z(v)\equiv\eta_0/\eta(v)$ with an obvious condition $0\le Z(v)\le 1$. Equations (5) can be rewritten as

$$\eta(v)\langle\mathbf{v}\rangle=\mathbf{F}_I, \tag{6}$$

where F_{Ix} and F_{Iy} are corresponding right-hand parts of Eqs. (5). From Eq. (6) we have

$$\eta(v)v=F_I, \tag{7}$$

where $F_I\equiv(F_{Ix}^2+F_{Iy}^2)^{1/2}$ and we omitted for simplicity the symbol of averaging for $\mathbf{v}$. Then from Eq. (7) follows that $v=v(F_I)$ and thus it is possible to represent $\eta_i(v)$ and $Z(v)$ in terms of F_I: $\eta_i(v)=\eta_i[v=v(F_I)]\equiv\tilde{\eta}_i(F_I)$ and

$$Z(v)=Z[v=v(F_I)]\equiv\nu_i(F_I). \tag{8}$$

Here $\nu_i(F_I)$ has a physical meaning of the probability to overcome the effective potential barrier of isotropic pinning under the influence of effective (v dependent through the $\tilde{\epsilon}$ dependence) force F_I. Then in terms of the $\nu_i(F_I)$, Eq. (6) takes the self-consistent form

$$\eta_0\mathbf{v}=\nu_i(F_I)\mathbf{F}_I, \tag{9}$$

which can be highly simplified for a small dimensionless Hall constant ($\epsilon\ll 1$). Really, in this limit $\tilde{\epsilon}=\epsilon\nu_i(F_i)$, where $F_i\equiv F_I(\epsilon=0)$ and the right-hand part of the Eq. (6) becomes v independent—i.e., is represented only in terms of the known quantities. Just in this limit all subsequent results of the paper will be discussed.

B. Nonlinear resistivity and conductivity tensors

The average electric field induced by the moving vortex system is given by

$$\mathbf{E}=(1/c)\mathbf{B}\times\mathbf{v}=n(B/c)(-v_y\mathbf{x}+v_x\mathbf{y}), \tag{10}$$

where $\mathbf{x}$ and $\mathbf{y}$ are the unit vectors in the x and y directions, respectively.

From formulas (9) and (10) we find the dimensionless magnetoresistivity tensor $\hat{\rho}$ (having components measured in units of the flux-flow resistivity $\rho_f\equiv\Phi_0B/\eta_0c^2$) for the nonlinear law $\mathbf{E}=\hat{\rho}(j)\mathbf{j}$:

$$\hat{\rho}=\begin{pmatrix}\rho_{xx} & \rho_{xy}\\ \rho_{yx} & \rho_{yy}\end{pmatrix}=\begin{pmatrix}\nu_i(F_I) & -n\epsilon\nu_i^2(F_i)\nu_a(F_{Lx})\\ n\epsilon\nu_i^2(F_i)\nu_a(F_{Lx}) & \nu_i(F_I)\nu_a(F_a)\end{pmatrix}. \tag{11}$$

The conductivity tensor $\hat{\sigma}$ (the components of which are measured in units of $1/\rho_f$), which is the inverse of the tensor $\hat{\rho}$, has the form

$$\hat{\sigma}=\begin{pmatrix}\sigma_{xx} & \sigma_{xy}\\ \sigma_{yx} & \sigma_{yy}\end{pmatrix}=\begin{pmatrix}[\nu_i(F_I)]^{-1} & n\epsilon\\ -n\epsilon & [\nu_i(F_I)\nu_a(F_a)]^{-1}\end{pmatrix}. \tag{12}$$

From Eqs. (11) and (12) we see that the off-diagonal components of the $\hat{\rho}$ and $\hat{\sigma}$ tensors satisfy the Onsager relation

($\rho_{xy}=-\rho_{yx}$ in the general nonlinear case and $\sigma_{xy}=-\sigma_{yx}$). All the components of the $\hat{\rho}$ tensor and the diagonal components of the $\hat{\sigma}$ tensor are functions of the current density j through the external force value F_L, the temperature T, the angle α, and the dimensionless Hall parameter ϵ. For the following (see Sec. II E 2) it is important, however, to stress that the off-diagonal components of the $\hat{\sigma}$ (i.e., the dimensional Hall conductivity terms $\delta=n\epsilon/\rho_f$) are not influenced by a presence of the i and a pins.[13]

The experimentally measurable resistive responses refer to a coordinate system tied to the current (see Fig. 1). The longitudinal and transverse (with respect to the current direction) components of the electric field, $E_\parallel$ and $E_\perp$, are related to E_x and E_y by the simple expressions

$$E_\parallel = E_x \sin\alpha + E_y \cos\alpha,$$

$$E_\perp = -E_x \cos\alpha + E_y \sin\alpha. \tag{13}$$

Then according to Eqs. (13), the expressions for the experimentally observable longitudinal and transverse (with respect to the **j** direction) magnetoresistivities $\rho_\parallel \equiv E_\parallel / j$ and $\rho_\perp \equiv E_\perp / j$ have the form

$$\rho_\parallel = \rho_{xx}\sin^2\alpha + \rho_{yy}\cos^2\alpha,$$

$$\rho_\perp = \rho_{yx} + (\rho_{yy} - \rho_{xx})\sin\alpha\cos\alpha. \tag{14}$$

Note, however, that the magnitudes of the $\rho_{\parallel,\perp}$, given by Eqs. (14), in general, depend on the direction of the external magnetic field **B** along z axis due to the $n\epsilon$ dependence of the F_I and F_a forces in arguments of the ν_i and ν_a functions, respectively. In order to consider only n-independent magnitudes of the $\rho_\parallel$ and $\rho_\perp$ resistivities we should introduce the even (+) and odd (−) magnetoresistivities with respect to magnetic field reversal ($\rho^\pm \equiv [\rho(n) \pm \rho(-n)]/2$) longitudinal and transverse dimensional magnetoresistivities, which in view of Eqs. (14) have the form

$$\rho_\parallel^+ = \rho_f[\sin^2\alpha + \nu_a(F_{Lx})\cos^2\alpha]\nu_i(F_i),$$

$$\rho_\parallel^- = \rho_f\{[\sin^2\alpha + \nu_a(F_{Lx})\cos^2\alpha]\nu_i^-(F_I) + \nu_i(F_i)\nu_a^-(F_a)\cos^2\alpha\}, \tag{15}$$

$$\rho_\perp^+ = -\rho_f\nu_i(F_i)[1-\nu_a(F_{Lx})]\sin\alpha\cos\alpha,$$

$$\rho_\perp^- = \rho_f(n\epsilon\nu_a(F_{Lx})\nu_i^2(F_i) + \{\nu_a^-(F_a)\nu_i(F_i) - \nu_i^-(F_I)[1-\nu_a(F_{Lx})]\}\sin\alpha\cos\alpha). \tag{16}$$

Here ν^- are the odd ($\nu^- \equiv \nu^-(n) = [\nu(n) - \nu(-n)]/2$) components of the functions $\nu_i(F_I)$ and $\nu_a(F_a)$, and for $\nu_a^-(F_a)$ we have the expansion in terms of $\epsilon \ll 1$:

$$\nu_a^- \simeq -n\epsilon\nu_i(F_i)F_{Ly}[d\nu_a(F_{Lx})/dF_{Lx}]. \tag{17}$$

Equations (15) and (16) are accurate to the first order in $\epsilon \ll 1$ and contain a lot of new physical information, which will be analyzed below (see Sec. II E). However, before this analysis it is instructive to discuss in short the main physically important features of two main limiting cases of purely anisotropic a pinning and isotropic i pinning, which follow from Eqs. (15) and (16), when $\nu_i=1$ or $\nu_a=1$, respectively.

C. Anisotropic *a* pinning

Setting $\nu_i=1$ we obtain rather simple formulas, which were derived first[11] for the experimentally observable nonlinear even and odd longitudinal and transverse anisotropic magnetoresistivities $\rho_{\parallel,\perp}^\pm(j,\theta,\alpha,\varepsilon_a)$ as functions of the transport current density j, dimensionless temperature θ and relative volume fraction $0 \le \varepsilon_a \le 1$, occupied by the parallel twin planes, directed at an angle α with respect to the current direction:

$$\rho_{\parallel a}^+ = \rho_f[\nu_a^+\cos^2\alpha + \sin^2\alpha], \quad \rho_{\perp a}^+ = \rho_f(\nu_a^+ - 1)\sin\alpha\cos\alpha, \tag{18}$$

$$\rho_{\parallel a}^- = \rho_f\nu_a^-\cos^2\alpha, \quad \rho_{\perp a}^- = \rho_f[n\epsilon\nu_a^+ + \nu_a^-\sin\alpha\cos\alpha]. \tag{19}$$

Here $\nu_a = \nu_a(F)$ is considered as the probability of overcoming the potential barrier of the washboard PPP in the x direction under the influence of the effective force $F \equiv F_{Lx} - n\epsilon F_{Ly}$.[11] This ν_a function describes an essentially nonlinear transition from the linear low-temperature thermoactivated flux-flow (TAFF) regime of vortex motion to the Ohmic FF regime. It is a steplike function of j or θ for a small fixed temperature or current density respectively (see Figs. 4 and 5 in Ref. 11).

It follows from Eqs. (18) and (19) that for $\alpha \neq 0, \pi/2$ the observed resistive response contains not only the ordinary longitudinal $\rho_{\parallel a}^+(\alpha)$ and transverse $\rho_{\perp a}^-(\alpha)$ magnetoresistivities, but also two new components induced by the pinning anisotropy: an *even transverse* $\rho_{\perp a}^+(\alpha)$ and an *odd longitudinal* component $\rho_{\parallel a}^-(\alpha)$. The physical origin of the $\rho_{\perp a}^+(\alpha)$ (which is independent of ϵ at $\epsilon \ll 1$) is related to the guided vortex motion along the "channels" of the washboard pinning potential in the TAFF regime. On the other hand, the component $\rho_{\parallel a}^-(\alpha)$ is proportional to the odd component ν_a^-, which is zero at $\epsilon=0$ and has a maximum in the region of the nonlinear transition from the TAFF to the FF regime at $\epsilon \neq 0$ (see Figs. 6 and 7 in Ref. 11). The (j,θ) dependence of the odd transverse (Hall) resistivity $\rho_{\perp a}^-(j,\theta)$ has contributions both from the even $\nu_a^+ \approx \nu_a$ and from the odd ν_a^- components of the $\nu_a(j,\theta)$ function. Their relative magnitudes are determined by the angle α and the dimensionless Hall constant ϵ. Note that as the odd longitudinal $\rho_{\parallel a}^-$ and odd transverse $\rho_{\perp a}^-$ magnetoresistivities arise by virtue of the Hall effect, their characteristic scale is proportional to $\epsilon \ll 1$ [see Eqs. (19)].

The appearance of these new odd Hall contributions follows from a guiding of the vortex along the channels of the washboard anisotropic pinning potential at $\alpha \neq 0, \pi/2$ and leads to the new specific angle-dependent scaling relations for the Hall conductivity[11] (in the limit $\epsilon \tan\alpha \ll 1$):

$$n\epsilon = (\rho_{\perp a}^- - \rho_{\parallel a}^-\tan\alpha)\cos^2\alpha/(\rho_{\parallel a}^+ - \rho_f\sin^2\alpha). \tag{20}$$

Here the dimensionless Hall constant $\epsilon \ll 1$ is uniquely related to three experimentally observable nonlinear resistivi-

ties $\rho^{+}_{\|a}, \rho^{-}_{\|a}, \rho^{-}_{\perp a}$ and the scaling relation (20) depends on the angle α. This relation differs substantially from the power-law scaling relations, obtained in the isotropic case[14] (see below). In the particular case $\alpha=0$ we regain the results,[10] specifically $\epsilon=\rho^{-}_{\perp a}/\rho^{+}_{\|a}$ (in Ref. 10, $\epsilon=\rho_{\perp}/\rho_{\|}$)—i.e., a linear relationship between $\rho^{-}_{\perp a}$ and $\rho^{+}_{\|a}$.

Equation (20) may be represented in another form

$$\rho^{-}_{\perp a}(\alpha) = \delta\nu_a(\alpha)\rho_f^2 - \rho^{-}_{\|a}(\alpha)\tan\,\alpha, \tag{21}$$

which is more suitable for considering scaling relations in longitudinal ($\alpha=\pi/2$) and transverse ($\alpha=0$) LT geometries of experiment.[11] In these geometries second term on the right-hand side of Eq. (21) is zero and we obtain that

$$\rho^{-}_{\perp a} = \tilde{\delta}(\rho^{+}_{\|a})^2, \tag{22}$$

$$\tilde{\delta}(\alpha=\pi/2) \equiv \tilde{\delta}_L = \delta\nu_a(0,\theta),$$

$$\tilde{\delta}(\alpha=0) \equiv \tilde{\delta}_T = \delta/\nu_a(j,\theta). \tag{23}$$

From Eqs. (22) and (23) follows that $\tilde{\delta}$ may be interpreted as an *effective* Hall conductivity in LT geometries which is suppressed for $\alpha=\pi/2$ ($\tilde{\delta}_L<\delta$) and enhanced for $\alpha=0$ ($\tilde{\delta}_T>\delta$) in comparison with a bare Hall conductivity δ. The physical reasons for this influence of the ν_a function on the $\tilde{\delta}$ behavior in LT geometries are simple and discussed in detail in Ref. 13.

D. Isotropic *i* pinning

For this case we put $\nu_a=1$ and from Eqs. (15) and (16) it follows that

$$\rho^{+}_{\|} = \rho_{\|i} = \rho_f\nu_i(F_L), \quad \rho^{-}_{\perp} = \rho_{\perp i} = \rho_f n\epsilon\nu_i^2(F_L), \tag{24}$$

where $F_L=F_i(\nu_a=1)=|\mathbf{F}_L|$. From Eqs. (24) the well-known scaling relation $\rho_{\|i}\sim(\rho_{\perp i})^2$, derived first in Ref. 14, follows. Note that $\rho^{+}_{\perp i}=\rho^{-}_{\|i}=0$ in this case; i.e., the nonlinear resistive response is isotropic.

E. Competition between *a* and *i* pinning

Equations (15) and (16) for the magnetoresistivities $\rho^{\pm}_{\|,\perp}$ at arbitrary value of competition between pointlike and anisotropic planar disorder for the in-plane geometry of experiment can be represented in a more suitable form, if we take into account Eqs. (18), (19), and (24):

$$\rho^{+}_{\|} = \nu_i(F_i)\rho^{+}_{\|a}, \quad \rho^{+}_{\perp} = \nu_i(F_i)\rho^{+}_{\perp a}, \tag{25}$$

$$\rho^{-}_{\|} = \nu^{-}_i\rho^{+}_{\|a} + \nu_i(F_i)\cdot\rho^{-}_{\|a}, \tag{26}$$

$$\rho^{-}_{\perp} = \rho_f n\epsilon\nu_a\nu_i^2 + \rho_f\{\nu^{-}_a\nu_i - \nu^{-}_i[1-\nu_a]\}\sin 2\alpha/2. \tag{27}$$

Here $\nu_i(F_i)$ is the probability function ν_i of anisotropic argument $F_i=[F_{Lx}^2\nu_a^2(F_{Lx})+F_{Ly}^2]^{1/2}$, the magnetoresistivity $\rho^{\pm}_{\|,\perp a}$, and the $\nu_a\equiv\nu_a(F_{Lx})$ functions in Eqs. (25)–(27) are the same as those in item C of Sec. II; $\nu^{-}_i=\nu^{-}_i[F_I(n)]$ and $F_I(n)=[F_{Ly}^2+F_{Lx}^2\nu_a^2(F_a)+2n\epsilon\nu_i(F_i)F_{Lx}F_{Ly}\nu_a(1-\nu_a)]^{1/2}$. It is easy to check, that previous results of Secs. II C and II D follow from Eqs. (25)–(27) in the limits of purely anisotropic (i.e., for $\nu_i=1$, $\nu^{-}_i=0$) and isotropic (i.e., for $\nu_a=1$, $\nu^{-}_a=0$) pins.

In this subsection it must be suffice to discuss in short the main physically important features of these equations. First of all, the magnetoresistivities $\rho^{\pm}_{\|,\perp}$ can be found if the ν_a and ν_i functions are known. Moreover, the converse statement is also valid: it is possible to reconstruct these functions from $(j,\,\theta,\,B)$-dependent resistive measurements, using only Eqs. (25), where the Hall terms are ignored. Equations (26) and (27), which arise due to the Hall effect, have a rather complicated structure, which reflects a more pronounced competition between isotropic and anisotropic disorder in the Hall-mediated resistive responses. Let us outline the main new physical results, following from Eqs. (25)–(27).

1. Pointlike disorder and vortex guiding

For the discussion of the influence of pointlike pins on the guiding of vortices in the anisotropic pinning potential it is sufficient to analyze Eqs. (25). Whereas for the purely anisotropic pinning ($\nu_i=1$) a critical current density j_c exists only for direction, which is strictly perpendicular to the PPP ($\alpha=0$) and $j_c(\alpha)=0$ for any other direction ($0<\alpha\leq\pi/2$) due to the guiding of vortices along the channels of a washboard potential, in Eqs. (25) the factor $\nu_i(F_i)$ ensures that an anisotropic critical current density $j_c(\alpha,\theta)$ exists for arbitrary angles α.

It is interesting, however, to note that the angular dependence of the ratio $\rho_{\perp}/\rho_{\|}$, which determines the angle β between **j** and **v** for *a* pins in Ref. 11, according to the relation

$$\cot\,\beta = -\frac{\rho^{+}_{\perp a}}{\rho_{\|a}} = \frac{1-\nu_a}{\tan\,\alpha + \nu_a\cot\,\alpha}, \tag{28}$$

is not influenced by the isotropic disorder, because factor $\nu_i(F_i)$ in Eqs. (25) vanishes from Eq. (28). Physically it means that the character of anisotropy in the case of competition between *i* and *a* pinning is determined only by $\langle\mathbf{F}^a_p\rangle=[\nu_a(F_{Lx},\theta)-1]\mathbf{F}_{Lx}$ (see Fig. 1)—i.e., by the average pinning force of the PPP. Isotropic pins influence only the magnitude of the average **v** vector, because $\langle\mathbf{F}^i_p\rangle\|\mathbf{v}\|\mathbf{F}_I$. So the polar resistivity diagram $\rho(\alpha)$, which can be measured experimentally,[5] is influenced by pointlike pins, because from Eqs. (11) it follows that

$$\rho(\alpha) = \rho_f[\rho_{xx}^2\sin^2\,\alpha + \rho_{yy}^2\cos^2\alpha]^{1/2}$$
$$= \rho_f\nu_i(F_i)(\sin^2\,\alpha + \nu_a^2\cos^2\,\alpha)^{1/2}. \tag{29}$$

2. New Hall voltages and scaling relations

As follows from Eqs. (26) and (27), the odd longitudinal $\rho^{-}_{\|}$ and transverse $\rho^{-}_{\perp}$ magnetoresistivities contain terms with the ν^{-}_i function. They possess a highly anisotropic current- and temperature-dependent bumplike behavior. They tend to zero in the linear regime of vortex motion. For $\alpha=0,\pi/2$ these new terms disappear, because $\nu^{-}_i=\nu^{-}_a=0$ at these limits. As was in the case of purely *a* pinning (see Sec. II C), the

appearance of these new odd Hall contributions follows from the emergence of a certain equivalence of xy directions due to a guiding of vortices along the channels of the washboard pinning potential for the case with $\alpha \neq 0, \pi/2$. Note also that $\rho_{\parallel}^{-}$ includes two terms with similar signs, whereas in $\rho_{\perp}^{-}$ there are terms with opposite signs. The latter can give rise to the well-known sign change in the (j,θ,H) dependence of the Hall resistivity below T_c.[12]

From Eqs. (25)–(27) new anisotropic scaling relations for the dimensionless Hall constant ϵ can be derived. For this purpose we exclude ν_i^- from Eqs. (25)–(27) and for ν_a^- use Eq. (17), and after some algebra in the limit $\epsilon \tan\alpha \ll 1$ we have

$$n\epsilon = \frac{2\rho_{\perp}^{-}\rho_{\parallel}^{+} + \rho_f \sin 2\alpha(1-\nu_a)\nu_i\rho_{\parallel}^{-}}{[2\nu_a\rho_{\parallel}^{+} - \sin 2\alpha\rho_f\nu_i F_{Ly}\nu_a']\rho_f\nu_i^2}. \tag{30}$$

It is easy to check that from Eq. (30) follows scaling relations $\delta = n\epsilon/\rho_f = \rho_{\perp i}/(\rho_{\parallel i})^2$ (for i pins at $\nu_a = 1$) and Eq. (20) (for a pins at $\nu_i = 1$).

As follows from Eqs. (25) and (27), just the same scaling relations as given by Eqs. (22) and (23) for a pins exist also for $(i+a)$ pins [with a replacement of corresponding a resistivities in Eq. (8) by $\rho_f\rho_{\perp}^{-}$ and $\rho_f\rho_{\parallel}^{+}$]. Physically it follows from the fact that point-like disorder influences only the magnitude of $\langle \mathbf{v} \rangle$ (Ref. 13) and does not change the angular dependence of the ratio $\rho_{\perp a}^{+}/\rho_{\parallel a}^{+}$, which determines the angle β between $\mathbf{j}$ and average velocity vector $\langle \mathbf{v} \rangle$ for a pins.[11]

III. GRAPHICAL ANALYSIS OF NONLINEAR REGIMES

A. Pinning potential and ν-function behavior

In order to analyze different types of nonlinear anisotropic (j,θ,α)-dependent magnetoresistivity responses, given by formulas (25)–(27), we should bear in mind that these responses, as is seen from formula (11), are completely determined by the (j,θ) behavior of the functions $\nu_a(F_a)$ and $\nu_i(F_i)$, having a sense of the probabilities to overcome the effective potential barriers of the a and i pins, respectively. A simple analytical model for the calculation of the (j,θ)-dependent ν functions was given earlier.[11,13,17] We will use for both ν_i and ν_a functions the one-dimensional periodic pinning potential $U_p(x)$ (see Fig. 2), which has a simple analytical form[11,17]

$$U_p(x) = \begin{cases} -F_p x, & 0 \leqslant x \leqslant b, \\ F_p(x-2b), & b \leqslant x \leqslant 2b, \\ 0, & 2b \leqslant x \leqslant h, \end{cases} \tag{31}$$

where F_p is the pinning force ($F_p = U_0/b$, where $U_0 > 0$ is the depth of the potential well and $2b$ is the width of the well). This form of $U_p(x)$ allows us to define as the properties of a given pinning center (by the parameters U_0 and b), as well as the density of such centers [by the parameter $\varepsilon = 2b/h$, where h is the period of the $U_p(x)$]. Calculation of the $\nu(j,\theta)$ function on the basis of the pinning potential, given by Eq. (31), was done.[11]

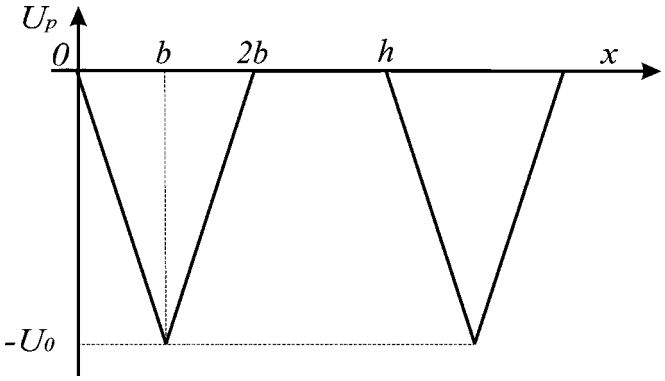

FIG. 2. Model pinning potential $U_p(x)$: h is the period of the potential, $2b$ is the width of the potential well, U_0 is the depth of the potential well, and $\varepsilon = 2b/h$ characterizes the concentration of the pinning planes.

The effect of the external force F acting on the vortices consists in a lowering of the potential barrier for vortices localized at pinning centers and, hence, an increase in their probability of escape from them. Increasing the temperature also leads to an increase in the probability to escape of the vortices from the pinning centers through an increase in the energy of thermal fluctuations of the vortices. Thus the pinning potential of a pinning center, which for $F, T \to 0$ leads to localization of the vortices, can be suppressed by both an external force and by temperature. A detailed quantitative and qualitative analysis of the behavior of $\nu(f,\theta,\epsilon)$ as a function of all the parameters and its asymptotic behavior as a function of each are described (see Figs. 4 and 5 in Ref. 11).

B. Dimensionless form of the $\rho_{\parallel,\perp}^{\pm}$ responses

Let us turn to the dimensionless parameters by which one can in general case take into account the difference of the potentials U_a and U_i—specifically the difference of their periods h_a, h_i, the potential well depths U_{0a}, U_{0i}, and the widths b_a, b_i. We introduce some new parameters: $\varepsilon = (\varepsilon_a\varepsilon_i)^{1/2}$ is the average concentration of pinning centers, $U_0 = (U_{0a}U_{0i})^{1/2}$ is the average depth of the potential well, $\kappa = (\varepsilon_i/\varepsilon_a)^{1/2} = (h_a b_i/h_i b_a)^{1/2}$, and $p = (U_{0a}/U_{0i})^{1/2}$, where the parameters κ and p are measures of the corresponding anisotropies. The temperature will be characterized by new parameters: $\theta_a = pT/U_0 = T/U_{0a}$ and $\theta_i = (1/p)T/U_0 = T/U_{0i}$, which are the ratio of the energy of thermal fluctuations of the vortices to the average potential well depth U_{0a} and U_{0i}, respectively.

The current density will be measured in units of $j_c = cU_0/\Phi_0 h$, where $h = (h_a h_i)^{1/2}$. Then the dimensionless parameters f_a and f_i, which specify the ratio of the external forces F_a and F_i to the pinning forces $F_{pa} = U_{0a}/b_a$ and $F_{pi} = U_{0i}/b_i$ (ν_a and ν_i are the even functions of their arguments), we denote as $f_a = F_a/F_{pa}$ and $f_i = F_i/F_{pi}$. The values of the external force F at which the heights of the potential barriers U_{0a} and U_{0i} vanish at $T=0$ correspond (at $\alpha=0$ and $\alpha = \pi/2$) to the critical current densities $j_{ca} = qj_c$ and $j_{ci} = j_c/q$, respectively, where $q = p/\kappa$. In the general case of nonzero temperature and $0 < \alpha < \pi/2$ it is possible to consider the

angle-dependent crossover current densities $j_{ca}(\alpha)$ and $j_{ci}(\alpha)$ (see below) which correspond to change in the vortex dynamics from the TAFF regime to a nonlinear regime. The condition that determines the temperature region in which the concept of critical current densities is physically meaningful is $0 \leqslant T \ll U_0$, because for $T \gtrsim U_0$ the transition from the TAFF to the nonlinear regime is smeared and the concept of critical current loses its physical meaning.

It is possible now to rewrite Eqs. (15) and (16) in dimensionless form in order to represent them as functions of j, θ, and α at given values of parameters ε, ϵ, q, and k; then, for anisotropic and isotropic moving forces at $\epsilon=0$ we have, respectively,

$$f_a = jq^{-1} \cos \alpha, \tag{32}$$

$$f_i = jq(\sin^2 \alpha + \nu_a^2 \cos^2 \alpha)^{1/2}. \tag{33}$$

Before following the graphical analysis of the $\rho_{\parallel,\perp}^{\pm}$ dimensionless dependences we should point out the magnitude of some parameters which will be used for the presentation of the graphs. It is important to remind the reader here that the parameter q determines the value of anisotropy between ν_i and ν_a critical current densities, whereas the parameter k describes the anisotropy magnitude of the width of nonlinear transition from the TAFF to the FF regime for the ν_i and ν_a functions. More definitely, if $q>1$, then $j_{ca}=qj_c>j_{ci}=j_c/q$ and influence of the i pins on the vortex dynamics decreases with q increasing. For $q<1$ the situation is opposite and anisotropy effects may be fully suppressed with q decreasing. So for the observation of pronounced competition between i and a pins $q \approx 1$ should be taken.

The temperature dependences of the $\rho_{\parallel}^{+}(\alpha)$ at small current densities under conditions of the presence both isotropic and anisotropic pinning potential were studied experimentally.[8] Arrhenius analysis of these dependences within the frames of suggested here theoretical approach have shown that for the samples[8] the $U_{0a}=4031$ K, $U_{0i}=1568$ K, $b_a=400$ nm, and $b_i=2000$ nm at $T \approx 8$ K. Then for these samples $q \approx 1.6$, $\kappa \approx 0.5$, and $\theta \approx 0.003$. It was also pointed out[8] that the best fitting of the experimental and theoretical curves was established for $b_i/b_a=15$, from which follows $\kappa \approx 0.25$. So for all graphs below we used $q=1.6$, $\kappa=0.25$, $\theta=0.003$, and $\epsilon=0.01$, and if it is not pointed out specifically, $\varepsilon_a=1$ and $\varepsilon_i=0.1$.

Note also that for the even longitudinal resistivity $\rho_{\parallel}^{+}$ and the even transverse resistivity $\rho_{\perp}^{+}$ for a small Hall effect, terms proportional to $\epsilon \ll 1$ are absent [see Eqs. (25)] and only contributions describing the competition between isotropic pinning and nonlinear guiding effects on the PPP in terms of the even ν_i and ν_a functions are presented.

C. Graphical analysis of current-angular dependences

1. (j,α) presentation of ν_a and ν_i

In order to discuss graphical (j,α) behavior of the resistive responses we will use ν_a and ν_i functions of their arguments f_a and f_i, respectively. Then these functions are, as a corresponding ν function,[11] the step functions in j (at fixed θ) or in θ (at fixed j). For every one of the ν functions it is useful to determine the "crossover current densities" $j_{ci}(\alpha)$ and $j_{ca}(\alpha)$ as those which correspond to the middle point of a sharp steplike nonlinear transition from the TAFF to the FF regime. As follows from Eqs. (32) and (33), we can present f_a and f_i as $f_a=j/j_{ca}(\alpha)$ with $j_{ca}(\alpha)=q/\cos\alpha$ and $f_i=j/j_{ci}(\alpha)$ with $j_{ci}(\alpha) \approx 1/q \cos\alpha$ for $\alpha \ll \pi/4$ and $j_{ci}(\alpha) \approx 1/\nu_a q \cos\alpha$ for $\tan^2\alpha \ll \nu_a^2(j,\alpha)$; $j_{ci}(\alpha) \approx 1/q \sin\alpha$ for $\alpha > \pi/4$ because Eq. (33) can be presented in two equivalent forms: namely, $f_i = jq \cos\alpha\sqrt{\tan^2\alpha+\nu_a^2}=jq \sin\alpha\sqrt{1+(\nu_a/\tan\alpha)^2}$.

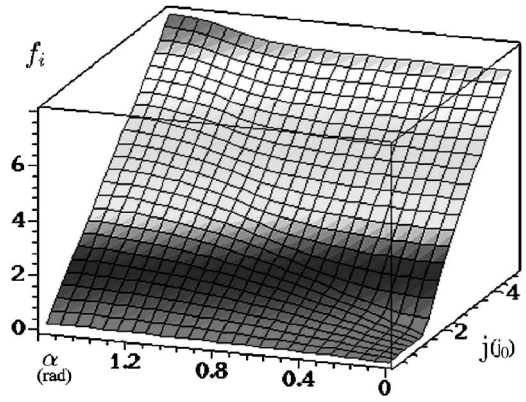

FIG. 3. The current-angle dependence of the average effective motive force for a vortex $f_i(j,\alpha)$.

The anisotropy of $f_i(\alpha)$ [see Eq. (33) and Fig. 3] can be divided into two types: simple ("external"), which depends on $\cos^2\alpha$, and more complex ("internal"), given by $\nu_a(\alpha)$. The first (external) anisotropy stems from the "tensorial" α dependence which exists also in the linear (TAFF and FF) regimes of the flux motion. The second (internal) is through the α dependence of ν_a, which in the region of transition from the TAFF to the FF regime is substantially nonlinear (see Fig. 4). The appearance of nonzero $\sin^2\alpha$ term in f_i for $\alpha \neq 0$ physically describes the guiding of vortices along the channels of the PPP in the presence of i pins for the current densities $j \lesssim j_{ci}(\alpha)$. The influence of ν_a anisotropy on ν_i is different for different values of the angle α (see Fig. 5). For

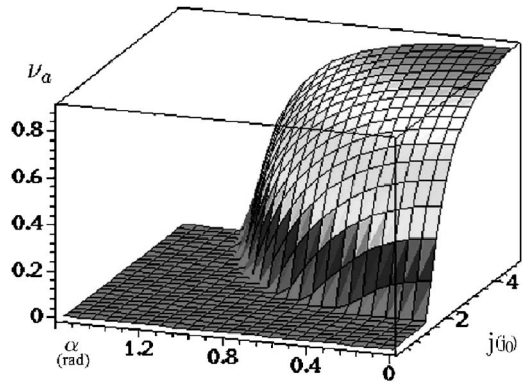

FIG. 4. The current-angle dependence of the anisotropic probability function $\nu_a(j,\alpha)$. In all following graphs the parameters $q=1.6$, $\kappa=0.25$, $\theta=0.003$, $\epsilon=0.01$, $\varepsilon_a=1$, and $\varepsilon_i=0.1$ (unless otherwise stated).

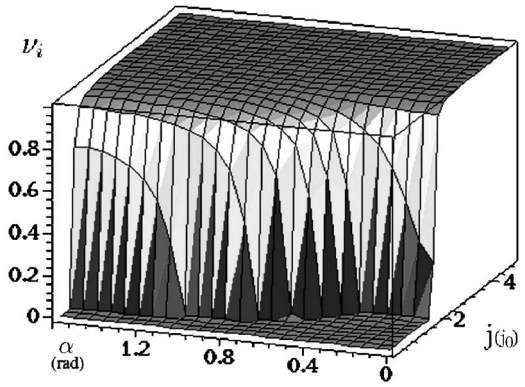

FIG. 5. The current-angle dependence of the isotropic probability function $\nu_i(j,\alpha)$.

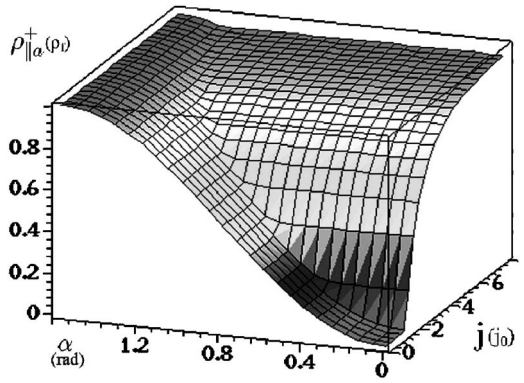

FIG. 6. The current-angle dependence of the dimensionless even longitudinal anisotropic magnetoresistivity $\rho^+_{\|a}(j,\alpha)$ for the value of the parameter $\varepsilon_a=1$.

$\alpha > \pi/4$ the anisotropy of $\nu_a(\alpha)$ does not influence the value of $f_i(\alpha)$ because $(\nu_a/\tan\alpha)^2 \ll 1$ in the expression for $j_{ci}(\alpha)$. On the contrary, for $\alpha \ll \pi/4$ the influence of a pins on $\nu_i(\alpha)$ is most effective for that range of current density, where $\nu_a^2 > \tan^2\alpha$, due to the inequality $\tan^2\alpha \ll 1$. Thus, the ν_i and ν_a as functions of the angle α at $j=$const behave themselves oppositely (see Figs. 4 and 5): ν_i increases monotonically with α increasing, whereas ν_a monotonically decreases. For $j \gtrsim j_{ca}(\alpha)$ and at small angles which meet the condition $\tan^2\alpha \ll 1$, the behavior of the ν_i and ν_a is qualitatively similar in α and opposite in q.

In the case where $\tan^2\alpha > 1$, the ν_i and ν_a behavior is qualitatively different and stems from the (α,q) dependences of the corresponding crossover current densities. In contradistinction to ν_a, the transition of ν_i from the TAFF to the FF depends weakly from α and q; it moves to the lower current densities with q increasing for $\alpha > \pi/4$ and moves to the higher ones for $\alpha \ll \pi/4$. In general, the ν_a behavior is more anisotropic than ν_i behavior. The ν_i anisotropy appears only in the TAFF regime, whereas ν_a anisotropy exists as in the TAFF, as well in the FF regime. And this anisotropy is greater in the current density as the angle α is greater. The ν_i and ν_a transition width at $\alpha=$const is defined by ε_i and ε_a parameters, respectively, and it increases for $\varepsilon_i \to 1$ and $\varepsilon_a \to 1$.

2. (j,α) presentation of even magnetoresistivities

Now we are in a position to discuss the results of the presentation of Eqs. (25) in the form of graphs. First we note that according to Eqs. (25), the even resistive responses can be represented as the products of corresponding isotropic and anisotropic ν functions. For this reason the graphical analysis of the $\rho^+_{\|}(j,\alpha)$ and $\rho^+_{\perp}(j,\alpha)$, after the above-mentioned consideration of the $\nu_i(j,\alpha)$ (see Fig. 5), can be reduced to the construction and analysis of the $\rho^+_{\|a}(j,\alpha)$ and $\rho^+_{\perp a}(j,\alpha)$ graphs.

Let us begin with a discussion of $\rho^+_{\|a}$ behavior [see Eq. (18) and Fig. 6]. For all $\alpha \neq 0$, due to the term $\sin^2\alpha$ in Eq. (18), a critical current density j_c exists only for direction, which is strictly perpendicular to the PPP ($\alpha=0$) (as was shown in Sec. II E 1) and $j_c(\alpha)=0$ for any other direction $(0 < \alpha \leq \pi/2)$ due to the guiding of vortices along the channels of a washboard potential (see also Fig. 8 in Ref. 11). In the FF regime the isotropization of the $\rho^+_{\|a}$ arises due to the vortex slipping over the PPP channels. Thus at small angles α the ν_a function strongly influences the $\rho^+_{\|a}$, whereas for $\alpha \to \pi/2$ this influence is not so effective due to the external anisotropy, which is proportional to the $\sin^2\alpha$ term.

Returning now to the consideration of the $\rho^+_{\|}(j,\alpha)$ graph we refer to Eqs. (25). It is necessary to pay special attention to the TAFF behavior of these curves at small currents and temperatures, which follows from the full pinning of vortices by pointlike pins. This behavior is completely different (for $\alpha \neq 0$) from the non-TAFF behavior of the corresponding graphs for the case of purely anisotropic pinning (see Fig. 8 in Ref. 11), which is provocated by the guiding of vortices along the channels of the PPP. At high current densities and (or) temperatures appears the FF regime, because the vortex motion transverse to the a-pins becomes substantial and longitudinal resistivity practically becomes isotropic. In these limiting cases the $\rho^+_{\|}(j)$ magnitudes are equal to unity (Fig. 7).

For the angles $0 < \alpha < \pi/2$ the $\rho^+_{\|}(j)$ behavior follows substantially the properties of one multiplier. The qualitative behavior of these multipliers, depending on the j and α magnitude, is very different as determined by different behavior of their crossover current densities j_{ci} and j_{ca}. The priority of

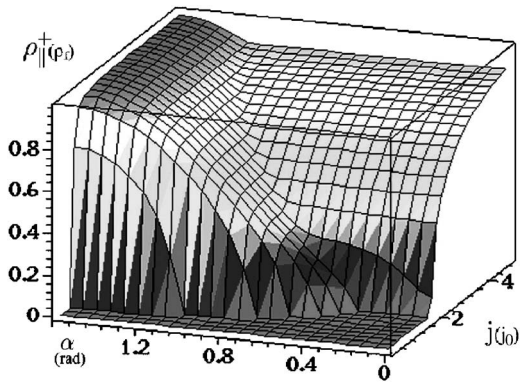

FIG. 7. The current-angle dependence of the dimensionless even longitudinal magnetoresistivity $\rho^+_{\|}(j,\alpha)$ for the value of the parameter $\varepsilon_a=1$.

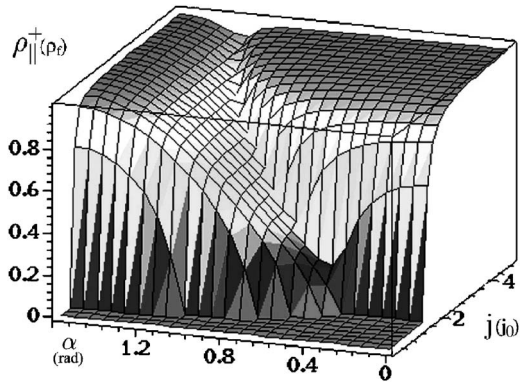

FIG. 8. The current-angle dependence of the dimensionless even longitudinal magnetoresistivity $\rho_{\parallel}^{+}(j,\alpha)$ for the value of the parameter $\varepsilon_a=0.01$.

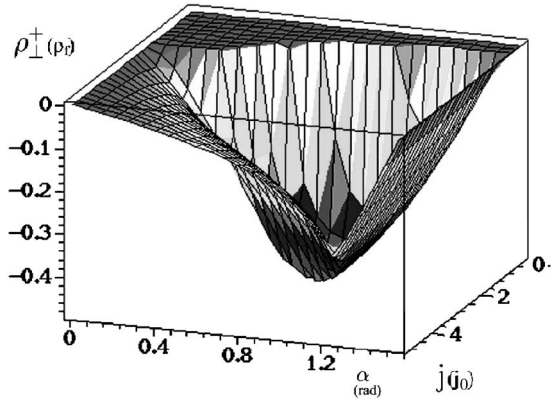

FIG. 9. The current-angle dependence of the dimensionless even transverse magnetoresistivity $\rho_{\perp}^{+}(j,\alpha)$. Pay attention to the inverted direction of the axes in comparison with Fig. 10.

a sharp rise of the appearance ν_i or ν_a functions depends on the competition between the crossover current densities j_{ci} and j_{ca}, respectively. That is why it may appear a "step" on some of the $\rho_{\parallel}^{+}(j)$ curves (for $q>1$ and $\alpha\neq 0,\pi/2$) when the next sequence of the vortex motion regimes is realized: (a) full i pinning in the TAFF regime ($0<j\lesssim j_{ci}$), (b) nonlinear transition from the TAFF to the FF regime for i pins ($j\gtrsim 2j_{ci}$), (c) practically linear the FF regime as a consequence of the guiding of vortices along the channels of the washboard PPP [on the $\rho_{\parallel}^{+}(j,\alpha)$ surface one can see the horizontal sections at $j\approx j_{ca}$; see Figs. 7 and 8], (d) nonlinear transition to the FF regime of vortex motion transverse to the a pins for $j\gtrsim j_{ca}$, and, at last, (e) a free FF motion for $j\gg j_{ca}$.

With decreasing of the q, (a)–(e) corresponding regions along the current density axis j can overlap each other and a common nonlinear transition appears instead of (b)–(d) regions. For the limiting cases $\alpha=0$, $\pi/2$, a guiding of vortices is absent and the $\rho_{\parallel}^{+}(j)$ LT behavior is simply related to the ν_i and ν_a behavior. If the parameter ε_a is decreasing, then the width of the transition of ν_a from the TAFF to the FF is also decreasing. Such an enhancement of the ν_a steepness leads to appearance of the minimum in α for the $\rho_{\parallel}^{+}(j,\alpha)$ graph (see Fig. 8).

Now we pass to a discussion of the $\rho_{\perp a}^{+}(j,\alpha)$ and $\rho_{\perp}^{+}(j,\alpha)$ graphs. Since the $\rho_{\perp}^{+}$, according to Eqs. (25), is the product of the $\rho_{\perp a}^{+}$ and $\nu_i(f_i)$, so this graph (see Fig. 9) can be reduced to the product of the graphs in Figs. 5 and 10. The transition from the TAFF to the FF regime is highly anisotropic in α; this causes a shift of the maximal $\rho_{\perp}^{+}(j,\alpha)$ magnitude in the direction of a small angle $\alpha\ll\pi/4$ for the j =const. That is why in view of the i pinning presence the $\rho_{\perp}^{+}(j,\alpha)$, as distinct from $\rho_{\perp a}^{+}(j,\alpha)$, has the minimum both in α and in j. This statement follows from the fact that influence of i pinning leads to $\rho_{\perp}^{+}\to 0$ for $0<j\lesssim j_{ci}(\alpha)$ due to $\nu_i\ll 1$. For the current densities $j\gtrsim j_{ca}(\alpha)$ the $\rho_{\perp}^{+}(j,\alpha)$ behavior is determined exclusively by the above-mentioned $\rho_{\perp a}^{+}(j,\alpha)$ behavior.

3. (j,α) presentation of odd magnetoresistivities

Before following discussion of the odd resistive responses we should remind the reader about the bumplike behavior of the current and temperature dependence of the ν^{-} functions (see Figs. 6 and 7 in Ref. 11), because the ν_i^{-} and ν_a^{-} functions give an important contribution to the odd responses. The $\nu^{-}(j)$ and $\nu^{-}(\theta)$ curves for the case of $\epsilon\ll 1$ in fact are proportional to the derivatives of the corresponding $\nu^{+}(j)$ and $\nu^{+}(\theta)$ curves, which have a steplike behavior as a function of their arguments [see Ref. 11 for the detailed discussion of this point and Eq. (17) in this paper]. As the $\rho_{\parallel}^{-}$ and $\rho_{\perp}^{-}$ resistivities given by Eqs. (26) and (27) arise by virtue of the Hall effect, their characteristic scale is proportional to $\epsilon\ll 1$, as for Eqs. (19) for purely anisotropic pins.

The position of the characteristic peak in the ν_i^{-} and ν_a^{-} functions is different for $q\neq 1$, because the parameter q determines the anisotropy of the critical current densities for i and a pins. So, if q is not very close to unity, the positions of the i and a peaks cannot coincide, and in this case the current and temperature odd resistive dependences $\rho_{\parallel,\perp}^{-}$ can have a bimodal behavior. For the $\rho_{\parallel}^{-}$ curves such dependences will correspond to existence of the resistive steps on the $\rho_{\parallel}^{+}$ curves (see Fig. 7), because for $\epsilon\ll 1$ we can consider the $\rho_{\parallel}^{-}$ dependences as derivatives of the $\rho_{\parallel}^{+}$curves. From this viewpoint it is easy to understand the previous assertion in Sec. II E 2 that $\rho_{\parallel}^{-}$ includes two terms (every proportional to the ν_i^{-} and ν_a^{-}, respectively) with similar signs.

Now let us discuss a graphical presentation of the Eq. (26), which can be represented as $\rho_{\parallel}^{-}=B_1+B_2$, where B_1

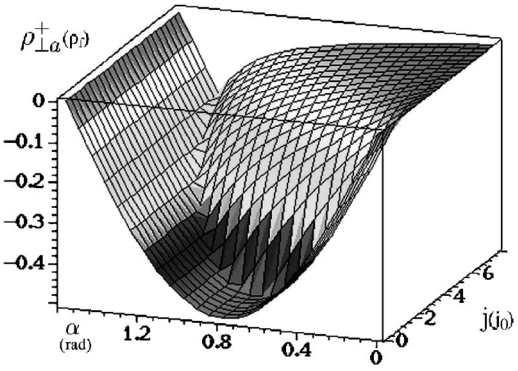

FIG. 10. The current-angle dependence of the dimensionless even transverse anisotropic magnetoresistivity $\rho_{\perp a}^{+}(j,\alpha)$.

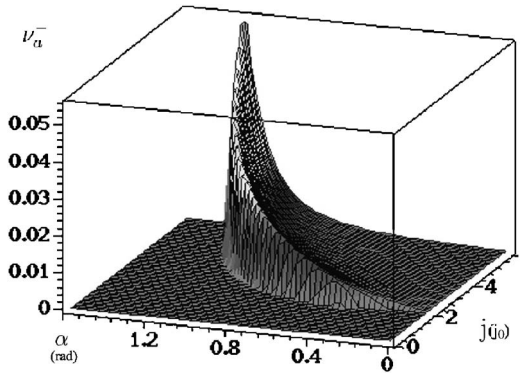

FIG. 11. The current-angle dependence of the function $\nu_a^-(j,\alpha)$.

$=\nu_i^-\rho_{\|a}^+$, and $B_2=\rho_f\nu_a^-\nu_i\cos^2\alpha$. Taking into account that every factor in the B_1 and B_2 is positive (see Figs. 5, 6, 11, and 12), we can conclude that $\rho_\|^-\geq 0$ for all values of the j,α,q.

The $\rho_\perp^-(j,\alpha)$ dependence is the most complicated. For the sake of simplicity the analysis we represent the $\rho_\perp^-$ as a sum $\rho_\perp^-=\rho_f[A_1+(A_2+A_3)\sin 2\alpha]$, where $A_1=n\epsilon\nu_a\nu_i^2$, $A_2=\nu_a^-\nu_i/2$, and $A_3=-\nu_i^-(1-\nu_a)/2$. First we consider the limiting cases of purely isotropic or anisotropic pinning ($\nu_a\to 1$ or $\nu_i\to 1$, respectively). For i pinning we have $\rho_\perp^-=\rho_f n\epsilon\nu_i^2$, from which follows (Vinokur *et al.*[14]) a scaling relation $\rho_\perp\sim\rho_\|^2$. For the case of purely anisotropic pinning $\rho_\perp^-=\rho_f\{n\epsilon\nu_a+(\nu_a^-\sin 2\alpha)/2\}$ and the scaling relation is $\rho_\perp\sim\rho_\|$ (see also Ref. 13).

Now we consider every term in the $\rho_\perp^-(j,\alpha)$ in detail. The A_1 contribution can be reduced in fact to the multiplication of the graph in Fig. 4 by the graph in Fig. 5 squared; the result is essentially nonzero for $j\geq j_{ca}(\alpha,q)$. The A_2 contribution was described above (see the B_2 term in the $\rho_\|^-$ without taking into account the $\cos^2\alpha$ anisotropy). Note also that both terms (A_1 and A_2) are positive for $n\epsilon>0$. The A_3 behavior is of great interest because the $A_3<0$ for $n\epsilon>0$. Let us consider the cases $q>1$ and $q<1$, which correspond to the a-, or i-pinning domination, respectively. Then, for $\alpha<\pi/4$, we have the following.

(a) For $q<1$ we have $j_{ci}(\alpha)>j_{ca}(\alpha)$ and the sharp maximum of the ν_i^- is suppressed by the factor $(1-\nu_a)\to 0$. As a result, the A_3 contribution can be ignored.

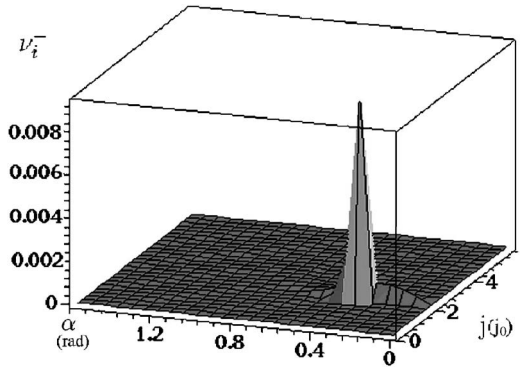

FIG. 12. The current-angle dependence of the function $\nu_i^-(j,\alpha)$.

(b) For $q\geq 1$ the opposite inequality follows—i.e., $j_{ci}(\alpha)<j_{ca}(\alpha)$. Then for $j\approx j_{ci}(\alpha)$ the A_3 term is dominant because $\nu_a\ll 1$ and $\nu_i^-\to n\epsilon$ in this (j,α) region (see Figs. 4 and 5). As a result, the $\rho_\perp^-(j,\alpha,q)$ change the sign for $j\approx j_{ci}(\alpha)$ and $0<\alpha\lesssim\pi/4$. Since the scale of the $\nu_i^-\ll\nu_i$, the amplitude of the minimum is small in comparison with the $\rho_\perp^-$ magnitude.

Thus, a competition of the a and i pinning leads to the qualitatively important conclusion that the $\rho_\perp^-$ can change its sign at a certain range of (α,j,q) values—namely, for $j\approx j_{ci}(\alpha,j,q)$, $0<\alpha\lesssim\pi/4$, and $q>1$.

D. Resistive response in a rotating current scheme

1. Polar diagram

An experimental study of the vortex dynamics in $YBa_2Cu_3O_{7-\delta}$ crystals with unidirectional twin planes was recently done using a modified rotating current scheme.[4,5] In that scheme it was possible to pass current in an arbitrary direction in the ab plane of the sample by means of four pairs of contacts placed in the plane of the sample. Two pairs of contacts were placed as in the conventional four-contact scheme, and the other two pairs were rotated by 90° with respect to the first (see the illustration in Fig. 1 of Ref. 4). By using two current sources connected to the outer pair of contacts, one can continuously vary the direction of the current transport in the sample. By simultaneously measuring the voltage in the two directions, one can determine directly the direction and magnitude of the average velocity vector of the vortices in the sample as a function of the direction and magnitude of the transport current density vector. This made it possible to obtain the angular dependence of the resistive response on the direction of the current with respect to the pinning planes on the same sample. The experimental data[4,5] attest to the anisotropy of the vortex dynamics in a certain temperature interval which depends on the value of the magnetic field. A rotating current scheme was used[4] to measure the polar diagrams of the total magnetoresistivity $\rho(\alpha)$, where $\rho=(\rho_x^2+\rho_y^2)^{1/2}$ is the absolute value of the magnetoresistivity, ρ_x and ρ_y are the x and$y$ components of the magnetoresistivity in an xy coordinate system, and α is the angle between the current direction and the oy axis (parallel to the channels of the a-pinning centers). In the case of a linear anisotropic response the polar diagram of the resistivity is an ellipse, as can easily be explained. In the case of a nonlinear resistive response the polar diagram of the resistivity is no longer an ellipse and has no simple interpretation.

In this subsection we carry out a theoretical analysis of the polar diagrams of the magnetoresistivity ρ in the general nonlinear case in the framework of a stochastic model of $a+i$ pinning. This type of angular dependence $\rho(\alpha)$ is informative and convenient for theoretical analysis. For a sample with specific internal characteristics of the pinning (such as q, ε_a, ε_i, and κ) at a given temperature and current density the function $\rho(\alpha)$ is contained by the resistive response of the system in entire region of angles α and makes it possible to compare the resistive response for any direction of the current with respect to the direction of the planar pinning centers. In addition, in view of the symmetric character of the

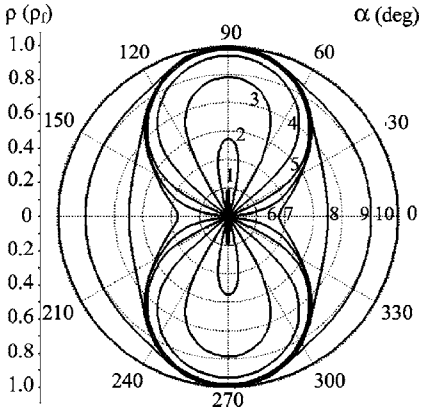

FIG. 13. Series of graphs of the function $\rho(\alpha)$ for a sequence of the parameter j: 0.63 (1), 0.65 (2), 0.75 (3), 1.00 (4), 1.50 (5), 1.92 (6), 2.00 (7), 2.50 (8), 4.00 (9), 20.0 (10) for $\varepsilon_a=1$.

$\rho(\alpha)$ curves, their measurements makes it possible to establish the spatial orientation of the system of the planar pinning centers with respect to the boundaries of the sample if this information is not known beforehand.

Now for analysis of the $\rho(\alpha)$ curves we imagine that vector **j** is rotated continuously from an angle $\alpha=\pi/2$ to $\alpha=0$. The characteristic form of the $\rho(\alpha)$ curves will obviously be determined by the sequence of dynamical regimes through which the vortex system passes as the current density vector is rotated. By virtue of the symmetry of the problem, the $\rho(\alpha)$ curves can be obtained in all regions of angles α from the parts in the first quadrant.

We recall that in respect to the two systems of pinning centers it is possible to have the linear TAFF and FF regimes of vortex dynamics and regimes of nonlinear transition between them. The regions of nonlinear transitions are determined by the corresponding values of the crossover current densities $j_{ci}(\alpha,q)$ and $j_{ca}(\alpha,q)$.

Now let us consider the typical $\rho(\alpha)$ dependences which are presented in Figs. 13 and 14 for a sequence of a current density magnitude. We remind that the polar diagram graphs represented below are constructed, as the previous graphs in

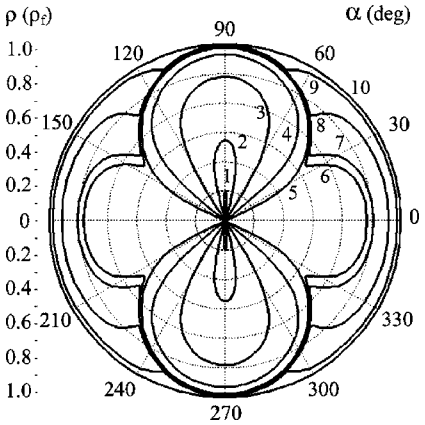

FIG. 14. Series of graphs of the function $\rho(\alpha)$ for a sequence of the parameter j: 0.63 (1), 0.65 (2), 0.75 (3), 1.00 (4), 1.50 (5), 1.92 (6), 2.00 (7), 2.50 (8), 4.00 (9), 20.0 (10) for $\varepsilon_a=0.1$.

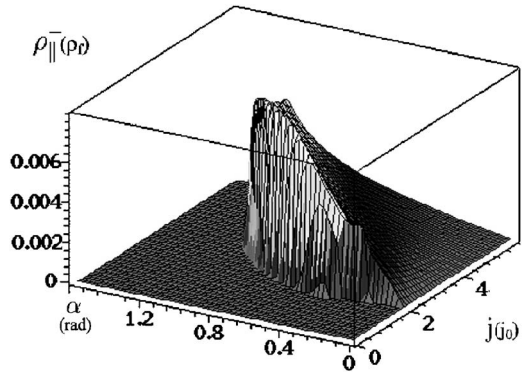

FIG. 15. The current-angle dependence of the odd longitudinal magnetoresistivity $\rho_{\parallel}^{-}(j,\alpha)$.

Figs. 3–7, 9–12, 15, and 16 for the next values of the parameters: $q=1.6$ (i.e., for the case with dominant a pins), $\kappa=0.25$, $\theta=0.003$, $\epsilon=0.01$, $\varepsilon_i=0.1$, $\varepsilon_a=1$ (Fig. 13), and $\varepsilon_a=0.1$ (Fig. 14). Note that $\rho(\alpha)$ is the product of two multipliers: one is the $\nu_i(f_i)$ dependence, which was earlier studied in Fig. 4 of Sec. III C 1, and other is the $\sqrt{\sin^2\alpha+\nu_a^2\cos^2\alpha}$ factor, which qualitative behavior is close to the $\rho_{\parallel a}^{+}(j,\alpha)$ dependence (see Fig. 6 in Sec. III C 2).

Let us analyze the $\rho(\alpha)$ behavior for the series of values of the current density j. When the angle α changes from 0 to $\pi/2$ the function $\rho(\alpha)$ grows monotonically from $\rho(0)=\nu_a(j/q)\nu_i(jq\nu_a(j/q))$ to $\rho(\pi/2)=\nu_i(jq)$. In Fig. 13 curves 1–6 of the function $\rho(\alpha)$ have the shape of a figure 8 drawn along the ox axis (strongly elongated for curves 1 and 2).

This anisotropy can be determined by the relation of the magnitudes of the half-axis at the direction $\alpha=\pi/2$ to the transverse half-axis for any fixed magnitude of the current density. Curves 1–6 of the $\rho=\rho(\alpha)$ graph have the figure-8 form elongated along the ox axis. It is caused by the steplike behavior of the ν_i function, corresponding for curves 1 and 2 to the crossover from the TAFF to the FF regime. That is why the magnitude of the $\rho(\pi/2)$ for curve 2 is rather greater than for the first one. With α increasing the ν_i function is in the TAFF region (see Fig. 5), which provocates the $\rho(\alpha)\ll 1$ in the case where the condition $j<j_{ci}(\alpha)$ is satisfied. Therefore, with j increasing the magnitude of the angle α, which separates the TAFF and FF regions of the ν_i function at a fixed value of the current density, decreases to the $\alpha\ll 1$.

As the $\nu_i(j,\alpha=\pi/2)$ is in the FF region [i.e., $j\gtrsim j_{ci}(\alpha=\pi/2)$], so the anisotropy of the figure-8 curve decreases for curves 3–6. The $\rho=\rho(\alpha)$ behavior of curves 5 and 6 is more isotropic in the region $\alpha\ll\pi/4$ than behavior of curves 1–4. If the condition $j>j_{ca}(0)$ is satisfied, an appearance of the nonzero resistance in corresponding region follows. Its magnitude is smaller than $\rho(\pi/2)$ for curves 7, 8, and 9 and practically is equal to the $\rho(\pi/2)$ for curve 10. Note that for the $\alpha=0,\pi$ and $j_{ca}<j\lesssim 3j_{ca}/2$ one can see the minimum, which decreases with j increasing and disappears in the case where the condition $j\gtrsim 3j_{ca}/2$ is satisfied. So for large magnitudes of the current densities the $\rho(\alpha)$ behavior becomes more isotropic.

It is necessary to pay attention to the $\rho=\rho(\alpha)$ behavior in the case where $\varepsilon_a=0,1$ (see Fig. 14) for the same series of

the magnitudes of the current densities. The behavior of curves 6, 7, 8, and 9 differs from the above-mentioned case, but the behavior of curves 1–5 and 10 remains the same. This fact is caused by the influence of the parameter ε_a on the ν_i behavior only in the area of its sharp steplike behavior at the $j \simeq j_{ca}(\alpha)$. Note that the ν_i contribution is dominant in the region $\alpha \ll 1$ as well as the above-mentioned anisotropy of the $\rho^+_{\perp a}(j,\alpha)$ (see Figs. 5 and 7). As decreasing of the ε_a causes the more narrow crossover from the TAFF to the FF regime, the $\nu_i(\alpha)$ has a minimum at fixed magnitude of the current density. The magnitude of this minimum decreases with the j increasing and the minimum shifts from the $\alpha \simeq \pi/4$ to the $\alpha \simeq \pi/2$. The influence of the parameter q acts on the crossover current densities j_{ci} and j_{ca} only quantitatively, but does not change an evolution of curves 1–10 qualitatively.

2. $\Theta_E(\alpha)$ dependence

Let us examine theoretically in our model a new type of the experimental dependence, recently studied[4] for $\Theta_E(\alpha)$, where Θ_E is the angle between the **j** vector and the electric field vector **E** measured at fixed values of the current density and temperature. Taking into account that in the xy coordinate system the magnetoresistivity components are $\rho_x = \rho_{xx}\sin\alpha = \nu_i(F_i)\sin\alpha$ and $\rho_y = \rho_{yy}\cos\alpha = \nu_i(F_i)\nu_a(F_a)\cos\alpha$, we obtain the following simple relation: $\tan\Theta_E(\alpha) = \rho_x/\rho_y = \tan\alpha/\nu_a(F_a)$ or

$$\Theta_E(\alpha) = \arctan[\tan\alpha/\nu_a(F_a)]. \tag{34}$$

Note that the ν_i term, describing the i pinning, is absent in Eq. (34). Then it follows from the latter that $\nu_a(j,\alpha,\theta) = \tan\alpha/\tan\Theta_E(j,\alpha,\theta)$; i.e., the $\nu_a(j,\alpha,\theta)$ function can be found from the experimental dependence $\Theta_E(\alpha)$. Unfortunately, the dependence $\Theta_E(\alpha)$ for the series of the temperature values was experimentally found[4] so far only for the FF regime (see Fig. 2 in Ref. 4). The $\Theta_E(j,\alpha)$ dependence is presented in Fig. 17. It shows all changes in the $\Theta_E(j,\alpha)$ behavior also for the TAFF regime.

Let us analyze Eq. (34) in detail. The $\Theta_E(j,\alpha)$ is the odd function of the angle α, and its magnitude increases monotonically with the α increasing for all values of the j due to the monotonical decreasing of the $\nu_a(j,\alpha)$ function (see Fig. 17). It follows from Eq. (34) that the period of the function $\Theta_E(\alpha)$ is equal to π. One more important limiting case is realized for $\nu_a \approx 1$, which corresponds to the limit of isotropic pinning. Depending on the inequality between the j magnitude and the crossover current density $j_{ca}(\alpha) \approx q/\cos\alpha$, one can separate two regions where the $\Theta_E(j,\alpha)$ behavior is qualitatively different. If A is the argument of the arctangent function in Eq. (34), then in that region j,α,q, where the inequality $j \gtrsim j_{ca}(\alpha)$ is true [the FF regime for $\nu_a(j,\alpha)$; see also Fig. 4], the magnitude of $\Theta_E \approx A$ as $A \ll 1$. And for the case $j \lesssim j_{ca}$ [the TAFF regime of the $\nu_a(j,\alpha)$] the value $\Theta_E \approx \pi/2 - A^{-1}$, as $A \gg 1$.

Note that the parameter ε_a influences the $\Theta_E(j,\alpha)$ by changing the character of the steplike crossover of the $\nu_a(j,\alpha)$ (the smaller the ε_a, the sharper the crossover). The value of the parameter q, as well as the above mentioned, determines the magnitude of the $j_{ca}(\alpha)$ [and therefore the position of the boundaries in j of the regions of quite different $\Theta_E(\alpha)$ behavior] at fixed α.

3. Critical current density anisotropy

Under the critical current density we mean the current density, which corresponds to the electric field strength on the sample $E = 1\ \mu\mathrm{V/cm}$. Let us determine the $j_c(\alpha)$ behavior graphically by crossing the $E^+_\parallel = j\rho^+_\parallel(j)$ graph and the plain $E = E_c$ in the polar coordinates. For all angles α the point of crossing for these graphs determines the critical current density magnitude for the defined direction and the crossing line of the graphs presents the dependence $j_c(\alpha)$.

Let us remind the reader that as in above-mentioned sections, in the nonlinear law $E^+_\parallel = j\rho^+_\parallel(j)$ we measure j and ρ in the values of the $j_0 = cU_0/\Phi_0 dh$ and $\rho_f = \rho_n B/B_{c2}$, respectively. That is why we have to measure the E magnitude in the $E_0 = j_0\rho_f$. As well as in Sec. III B we use the data from Ref. 8, where for the niobium samples $\rho_n \approx 5.5 \times 10^{-6}\ \Omega\,\mathrm{cm}$, $B \approx 150\ \mathrm{G\,s}$, $B_{c2} \approx 17\ \mathrm{kG\,s}$, $\rho_f \approx 5 \times 10^{-8}\ \Omega\,\mathrm{cm}$, $U_0 = 2500\ \mathrm{K}$, and $d = 2.5 \times 10^{-6}\ \mathrm{cm}$.

Therefore, $E_0 \approx 6 \times 10^{-6}\ \mathrm{V/cm}$, and for $E_c = 1\ \mu\mathrm{V/cm}$ we have to cross the dimensionless $\rho^+_\parallel(j)j$ graph by the plain $E \approx 0.002$.

Now we will discuss the $j_c(\alpha)$ as a function of α, q, E_c, and ε in detail. The $j_c(\alpha)$ anisotropy can be determined by the relation of the magnitudes of the half-axis at the direction $\alpha = 0$ to the transverse half-axis for any fixed magnitude of the parameters q and E_c. The $j_c(\alpha)$ decreases monotonically from $j_c(0)$ with α increasing and has a minimum for $\alpha = \pi/2$. It is caused by the fact that, as was shown in Sec. II C 1, the a pinning (with high values of the j_{ca} for $q > 1$) does not influence the i pinning for $\alpha = \pi/2$. Therefore, the inequality for the crossover current densities $j_{ci}(\alpha) < j_{ca}(\alpha)$ for $q > 1$ leads to the corresponding inequality for the critical current densities $j_c(0) < j_c(\pi/2)$.

The q influences the $j_c(\alpha)$ behavior (as in Sec. II D 1) only quantitatively: with q increasing the ratio $j_c(0)/j_c(\pi/2)$ grows and vice versa. It is caused by the $j_c(0)$ increasing and $j_c(\pi/2)$ decreasing due to the α behavior of the corresponding crossover current densities $j_{ci}(\alpha)$ and $j_{ca}(\alpha)$. The smaller the ε_a, the sharper the crossover between the $j_c(\alpha)$ regions of slowly and quickly decreasing as a function of the α. With E_c increasing the nonlinear law $E^+_\parallel = \rho^+_\parallel(j)j$ is satisfied for the larger values of the current density.

That is why with α increasing from 0 to α^* values [for which the condition $\tan^2\alpha^* \ll \nu_a^2(j,\alpha^*)$ is satisfied] the ν_a function is in the FF regime and $j_c(\alpha)$ decreases slowly. When the condition $\alpha > \alpha^*$ is true the ν_a function has a steplike crossover from the FF to the TAFF regime and $j_c(\alpha)$ decreases quickly.

So the α^* behavior as a function of the parameters q and E_c is qualitatively different: it increases with E_c increasing and decreases with q increasing. On the increase of the E_c by several orders of magnitude the $j_c(\alpha)$ curve degenerates into a circumference due to the isotropization of the $j_{ci}(\alpha)$ and $j_{ca}(\alpha)$ behavior for the high j values. Otherwise, with E_c decreasing the $j_c(\alpha)$ curve degenerates into a narrow loop,

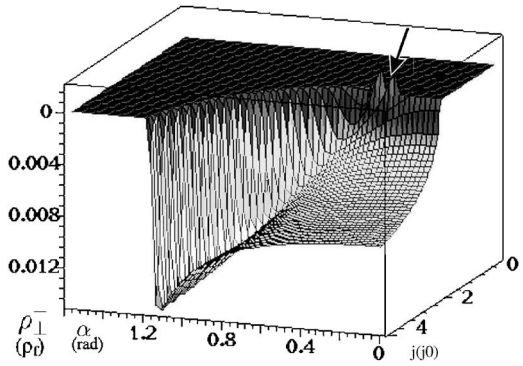

FIG. 16. The current-angle dependence of the odd transverse magnetoresistivity $\rho_\perp^-(j,\alpha)$. The characteristic minimum (which is shown by the arrow) is in the region $0<\alpha<\pi/4$ and $j\approx j_{ci}(\alpha)$. The minimum is shown as two neighboring minimums due to the steplike behavior of the calculation. Pay attention to the inverted direction of the axes in comparison with Fig. 15.

because the $j_{ci}(\alpha)$ and $j_{ca}(\alpha)$ behavior for a small j is very anisotropic.

IV. CONCLUSION

In the present work we have theoretically examined the strongly nonlinear anisotropic two-dimensional single-vortex dynamics of a superconductor with coexistence of the anisotropic washboard PPP and isotropic pinning potential as function of the transport current density j and the angle α between the direction of the current and PPP planes at a fixed temperature θ.

The experimental realization of the model studied here can be based on both naturally occurring[2–5] and artificially created[6–8] systems with $(i+a)$-pinning structures. The proposed model has made it possible for the first time (as far as we know) to give a consistent description of the nonlinear anisotropic current- and temperature-induced depinning of vortices for an arbitrary direction relative to the anisotropy of the washboard PPP. In the framework of this model one can successfully analyze theoretically certain observed resistive responses which are used for studying anisotropic pinning in

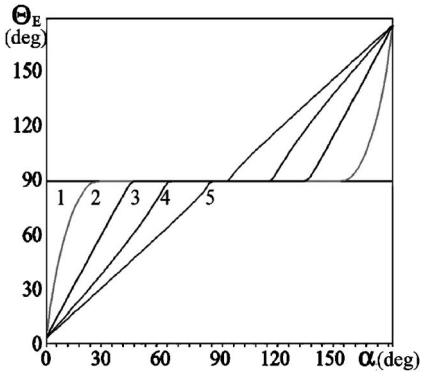

FIG. 17. Series of graphs of the function $\Theta_E(\alpha)$ for a sequence of the parameter j: 1 (1), 1.7 (2), 2.2 (3), 3.5 (4), 20 (5) for $T=8$ K.

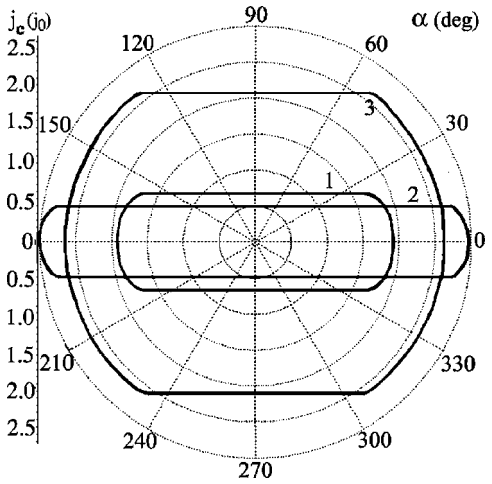

FIG. 18. Series of graphs of the function $j_c(\alpha)$ for the parameter pairs: $E_c=0.002$, $q=1.6$ (1); $E_c=0.002$, $q=3$ (2); $E_c=2$, $q=1.6$ (3).

a number of new experimental techniques[4] [the polar diagram of $\rho(\alpha)$, the $\Theta_E(\alpha)$ curve described by formula (34)] as well as new Hall responses specific for the $(i+a)$-pinning problem.

A quantitative description of the anisotropic nonlinear resistive properties of the problem under study is done in the framework of the stochastic model on the basis of the Fokker-Planck approach. The main nonlinear components of the problem are the anisotropic $\nu_a(F_a)$ and isotropic $\nu_i(F_i)$ probability functions for the vortices to overcome the potential barriers of a- and i-pinning centers under the action of anisotropic motive forces F_a and F_i, respectively. The latter include both the "external" parameters j,α, and θ and the "internal" parameters q, ε_i, and ε_a which describe the intensity and anisotropy of the pinning. As can be seen from Eqs. (25)–(27), the magnetoresistivities $\rho_{\parallel,\perp}^{\pm}(j,\alpha,\theta)$ are, in general, nonlinear combinations of the experimentally measured ν_i and ν_a functions (ν_i can be measured independently from the $\rho_{\parallel,\perp}^{+}(\alpha=\pi/2)$ [see Eq. (25)] and ν_a from the $\Theta_E(\alpha)$ [see Eq. (34)]).

Therefore, the nonlinear (in j) resistive behavior of the vortex system can be caused by factors of both an anisotropic and isotropic pinning origin. It is important to underline that whereas the structure of the $\nu_a(F_a)$ and F_a is the same as for purely a-pinning problem, the structure of the $\nu_i(F_i)$ and F_i is strongly different from the structure of the purely i-pinning problem due to the fact that F_i, as motive force of the $i+a$ problem, is nonlinear and anisotropic [see Eqs. (32) and (33)] and [Figs. 3–5].

Two main new features appear due to the introduction of the isotropic i pins into the initially anisotropic a-pinning problem. First, unlike the stochastic model of uniaxial anisotropic pinning studied previously,[10,11] where the critical current density j_c is indeed equal to zero for all directions (excepting $\alpha=0$) due to the guiding of vortices, in the given $i+a$ model the anisotropic critical current density $j_c(\alpha)$ exists for all directions because i pins "quench" the guiding of vortices in the limit $(j,\theta)\to 0$. Second, the Hall resistivity response functions $\rho_\perp^-(j,\alpha)$ can have a change of sign in a

certain range of (j,α,q) (at fixed dimensionless Hall constant $\epsilon=\alpha_H/\eta$ and the dimensional Hall conductivity $\delta=n\epsilon/\rho_f$), whereas the sign of the $\rho_{\|}^{-}(j,\alpha)$ does not change.

It should be noted that recently[8] the nonlinear (in θ) anisotropic longitudinal and transverse resistances of Nb films deposited on facetted sapphire substrates were measured at different angles α between **j** and facet ridges in a broad range of temperature and relatively small magnetic field **H**. The experimental data were in good agreement with the theoretical model described here. The measured $\rho_{\|}^{+}(\theta,\alpha)$ dependences can be fitted using the probability functions ν_a and ν_i in the form proposed here [see Eq. (25)] with the anisotropic and isotropic pinning potential given by Eq. (25). The periods and depths of the potential wells were estimated from the experimental data[8] and were used here (see Sec. III) for the theoretical analysis of different types of nonlinear anisotropic (j,α)-dependent magnetoresistivity responses, given by Eqs. (25)–(27), in the form of graphs (see Figs. 3–18). Whether these theoretical results can explain a new portion of the (j,α)-dependent $i+a$ resistivity data measured at $\theta=$const (in particular, for the samples investigated earlier[8] at small current densities) remains to be seen.[18–20]

[1] A. K. Niessen and C. H. Weijsenfeld, J. Appl. Phys. **40**, 384 (1969).
[2] A. A. Prodan *et al.*, Physica C **302**, 271 (1998).
[3] V. V. Chabanenko *et al.*, Physica C **314**, 133 (1999).
[4] H. Pastoriza, S. Candia, and G. Nieva, Phys. Rev. Lett. **83**, 1026 (1999).
[5] G. D'Anna, V. Berseth, L. Forro, A. Erb, and E. Walker, Phys. Rev. B **61**, 4215 (2000).
[6] M. Huth *et al.*, Adv. Funct. Mater. **12**, 333 (2002).
[7] O. K. Soroka *et al.*, Physica C **388-389**, 773 (2003).
[8] O. K. Soroka, Ph.D. thesis, J. Gutenberg University, Mainz, 2005.
[9] O. K. Soroka *et al.* (unpublished).
[10] Y. Mawatari, Phys. Rev. B **56**, 3433 (1997).
[11] V. A. Shklovskij, A. A. Soroka, and A. K. Soroka, Zh. Eksp. Teor. Fiz. **116**, 2103 (1999) [JETP **89**, 1138 (1999)].
[12] G. Blatter *et al.*, Rev. Mod. Phys. **66**, 1125 (1994).
[13] V. A. Shklovskij, J. Low Temp. Phys. **139**, 289 (2005).
[14] V. M. Vinokur, V. B. Geshkenbein, M. V. Feigel'man, and G. Blatter, Phys. Rev. Lett. **71**, 1242 (1993).
[15] O. V. Usatenko and V. A. Shklovskij, J. Phys. A **27**, 5043 (1994).
[16] V. A. Shklovskij, Phys. Rev. B **65**, 092508 (2002).
[17] V. A. Shklovskij and A. A. Soroka, Fiz. Nizk. Temp. **28**, 365 (2002); [Low Temp. Phys. **28**, 254 (2002)].
[18] V. A. Shklovskij, J. Low Temp. Phys. **130**, 407 (2003).
[19] V. A. Shklovskij, Physica C **388-389**, 655 (2003).
[20] B. Chen and J. Dong, Phys. Rev. B **44**, 10206 (1991).